Broad iron Kα line in Cygnus X-1 Simultaneously seen by *XMM-Newton* , *RXTE* & *INTEGRAL*

Refiz Duro[1], Thomas Dauser[1], Jörn Wilms[1], Victoria Grinberg[1]
Jérôme Rordriguez[7], Katja Pottschmidt[6], Maria Diaz-Trigo[4], Sonja Fritz[1,2]
Eckhart Kendziorra[2], Marcus Kirsch[3], Rüdiger Staubert[2], Michael A. Nowak[5]

[1] ECAP, [2] IAAT, [3] ESA-ESOC, [4] ESO, [5] MIT, [6] CRESST/UMBC/NASA-GSFC, [6] CEA Saclay
refiz.duro@sternwarte.uni-erlangen.de

Abstract

We report on the analysis of the broadened, fluorescent iron $K\alpha$ line in 4 sets of simultaneous *XMM-Newton* , *RXTE* and *INTEGRAL* observations of Cygnus X-1. The *XMM-Newton* data were taken in Modified Timing Mode of the EPIC-pn camera, while *RXTE* and *INTEGRAL* data provided the constraints on the continuum parameters. The best-fit spectrum consists of the sum of an exponentially cut-off power-law and a relativistically smeared, ionized reflection. Assuming a standard, thin accretion disk, the black hole in Cygnus X-1 has an angular momentum that is close to maximum.

Source behaviour

For our data analysis we include *RXTE* data which is strictly simultaneous to *XMM-Newton* data, as seen in Fig. 3. When it comes to *INTEGRAL* (IBIS) data (see Fig. 1) we encounter three situations to chose from: 1) strictly simultaneous data, 2) same state data and 3) same flux level data.

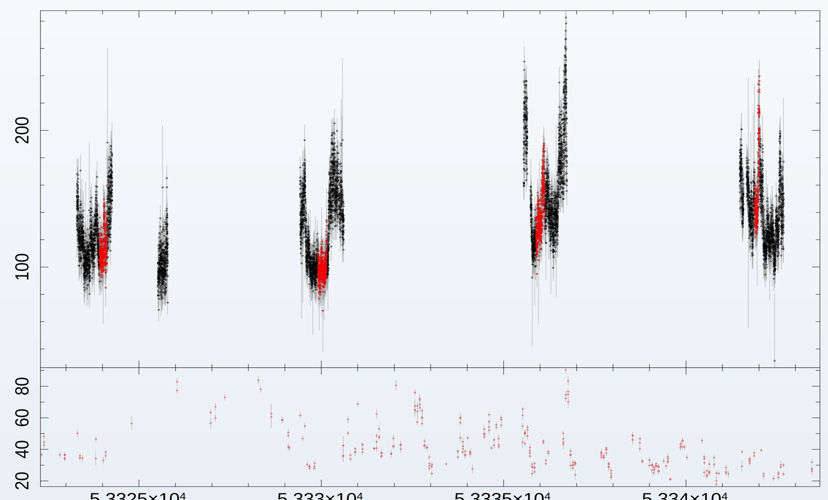

Figure 1: Upper pannel shows 40 second binned IBIS data. Red part shows strictly simultaneous data with XMM-Newton data. Using all of the data (black and red) produces misalignment with HEXTE data. Lower pannel shows ASM lightcurve.

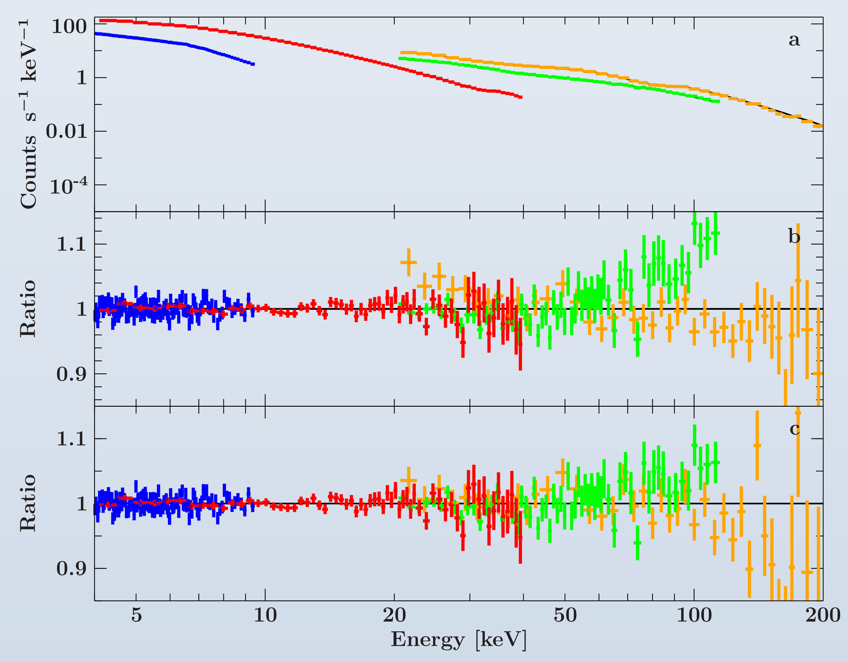

Figure 2: Join fit of *EPIC-pn*, *PCA* , *HEXTE* and *IBIS* data. The disagreement between the HEXTE and total IBIS data is clearly seen in pannel b, while it is mostly removed by using the same flux IBIS data in pannel c.

The first situation does not provide us with enough data (only up to ~ 15 ks for each observation), second one introduces disagreement with *RXTE* data, which is possibly due to the flux variability in the *INTEGRAL* data, while the third situation gives us enough exposure time (factor of ~ 5 compared to first situation) and agreement with *RXTE* data (see Fig. 2).

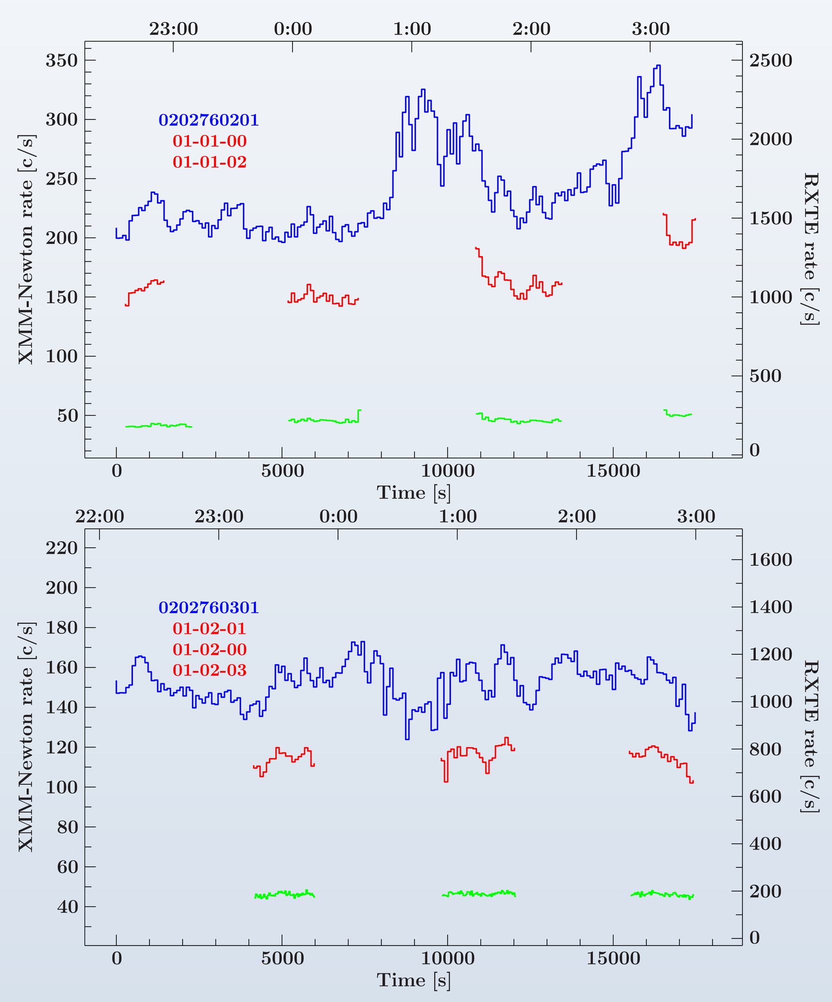

Figure 3: Thick filter *EPIC-pn*, top layer, PCU2 *PCA* and *HEXTE* background subtracted lightcurves for 2 observations. The lower pannel data has been studied by Duro et al. 2011.

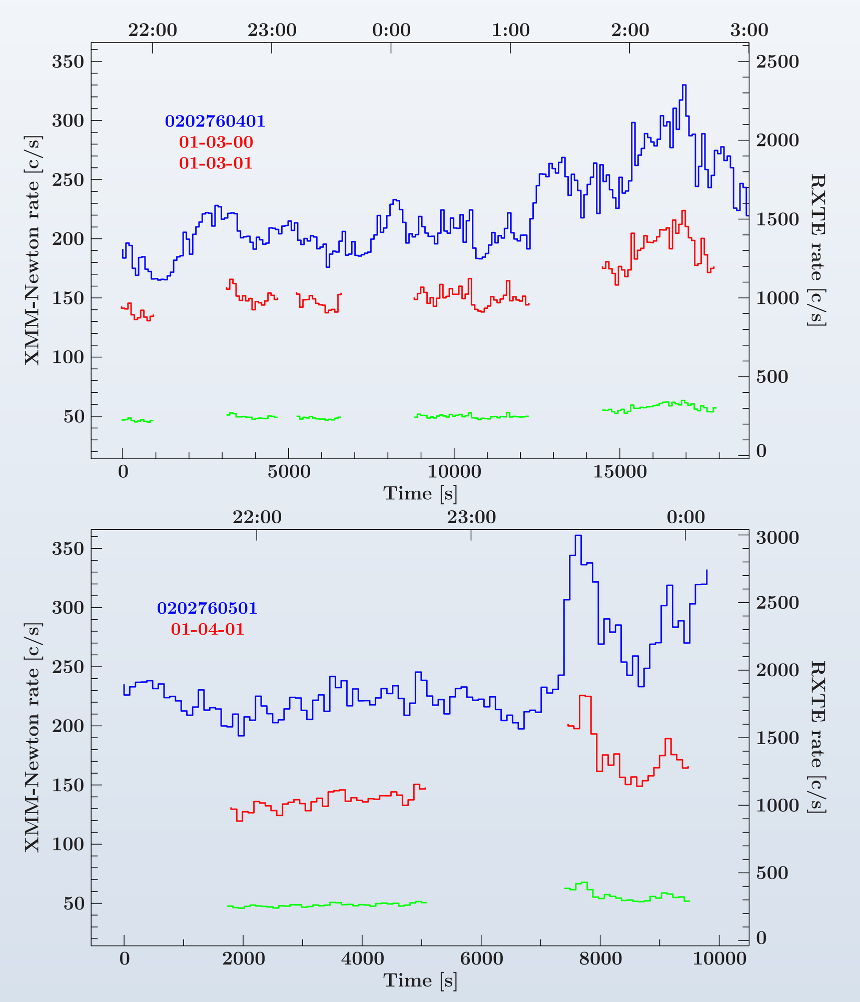

Figure 4: Thick filter *EPIC-pn*, top layer, PCU2 *PCA* and *HEXTE* background subtracted lightcurves for 2 observations.

Spectral properties

Based on the model used by Duro et al. 2011 (where observation 0202760301 was analysed), we fit the spectrum now extending to energies of few hundreds keV. Hence, we expect to constrain continuum parameters better, and likewise the reflection features parameters. The fits to the data shown in Fig. 5 describe Cygnus X-1 as moderately ionized, with high iron abundancy, but also with differing spin values.

$$\textbf{Const} \star \textbf{gabs} \star (\textbf{cutoffpl} + \textbf{diskbb} + \textbf{gauss} + (\textbf{relconv} \otimes \textbf{reflionx}))$$

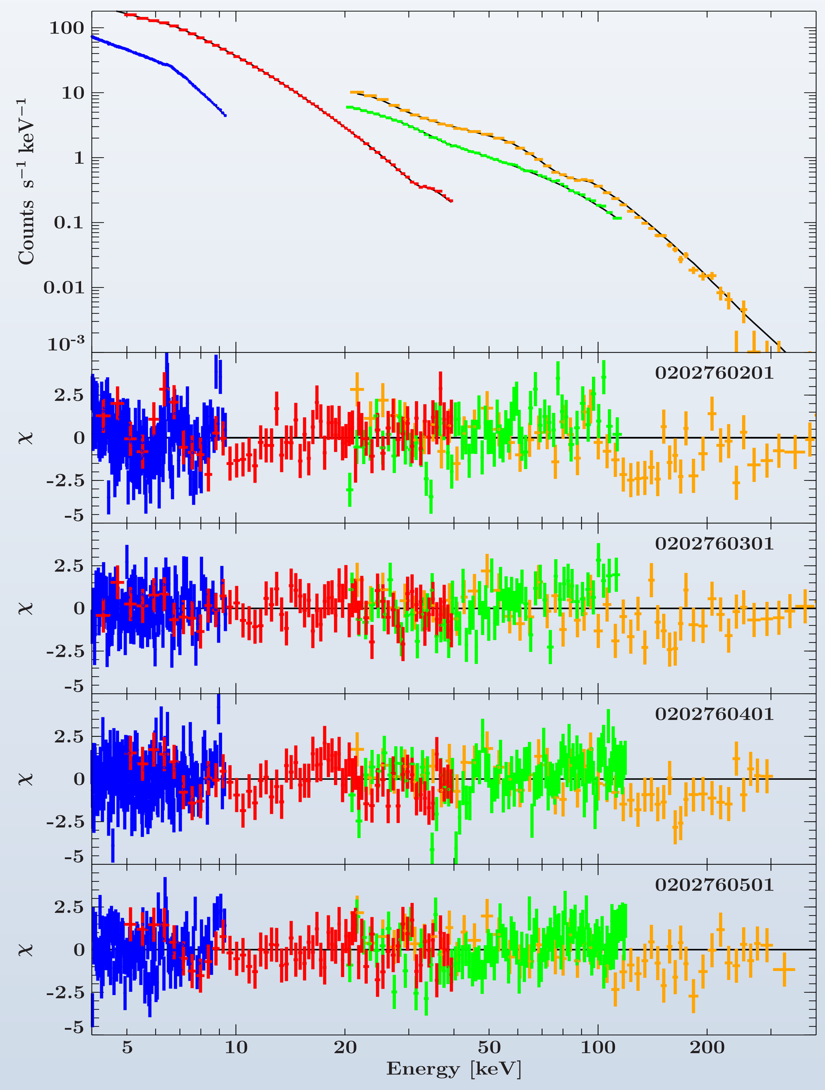

Figure 5: Best fit residuals for all four observations, when same flux level IBIS data is used. Residuals still show a need for better modeling, possibly with more physical models as for example is *eqpair* as is used in Cadolle et al. 2006.

The high spin value emerges for the thin disk solution with the typical emission profile value $\epsilon = 3$. Low spin value is prefered only when ϵ gets higher values, which means that the broad iron line is generated by strongly concentrating all available emmisivity to the innermost regions of a disk around a Schwarzschild black hole. This situation is highly unlikely, so the low ϵ, high spin value solution is prefered. This is consistent with spin measurements from the accretion disk continuum (Gou et al. 2011). We also get low spin for thin disk solution, but only when the inclination of the system is too low which is in disagreement with Sowers et al. 1998 and Davis & Hartmann 1983 for the inclination measurements.

0202760201	ϵ free	ϵ frozen
Γ_{pl}	1.738 ± 0.010	$1.732^{+0.010}_{-0.013}$
E_{fold} [keV]	229^{+20}_{-18}	221^{+20}_{-17}
ξ [erg cm s^{-1}]	$(2.9 \pm 0.2) \times 10^3$	$\left(2.91^{+0.35}_{-0.23}\right) \times 10^3$
Fe/Fe$_\odot$	$2.5^{+0.5}_{-0.4}$	$3.0^{+0.6}_{-0.5}$
a	$0.12^{+0.08}_{-0.06}$	$0.99^{+0.00}_{-0.05}$
i[deg]	$37.5^{+0.8}_{-0.6}$	$33.7^{+2.0}_{-1.6}$
ϵ	10^{+0}_{-5}	3
χ^2/dof	606/350	695/351

0202760401	ϵ free	ϵ frozen
Γ_{pl}	1.609 ± 0.010	$1.605^{+0.009}_{-0.014}$
E_{fold} [keV]	177^{+10}_{-9}	185^{+10}_{-12}
ξ [erg cm s^{-1}]	$\left(2.40^{+0.39}_{-0.18}\right) \times 10^3$	$\left(2.40^{+0.39}_{-0.18}\right) \times 10^3$
Fe/Fe$_\odot$	$3.4^{+0.9}_{-0.8}$	$2.8^{+0.8}_{-0.6}$
a	$0.04^{+0.26}_{-0.39}$	$0.40^{+0.20}_{-0.27}$
i[deg]	$32.6^{+2.7}_{-3.1}$	$26.1^{+2.6}_{-3.9}$
ϵ	$4.6^{+1.9}_{-0.9}$	3
χ^2/dof	550/396	560/397

0202760301	ϵ free	ϵ frozen
Γ_{pl}	$1.617^{+0.012}_{-0.015}$	$1.613^{+0.017}_{-0.016}$
E_{fold} [keV]	170^{+12}_{-11}	170^{+13}_{-11}
ξ [erg cm s^{-1}]	$(2.0 \pm 0.3) \times 10^3$	$\left(2.10^{+0.3}_{-0.4}\right) \times 10^3$
Fe/Fe$_\odot$	$3.0^{+0.9}_{-0.6}$	$3.3^{+1.1}_{-0.8}$
a	$-0.2^{+0.3}_{-0.4}$	$0.87^{+0.08}_{-0.12}$
i[deg]	33.3 ± 2.0	29^{+2}_{-3}
ϵ	8 ± 2	3
χ^2/dof	347/289	356/290

0202760501	ϵ free	ϵ frozen
Γ_{pl}	1.572 ± 0.010	$1.564^{+0.010}_{-0.009}$
E_{fold} [keV]	161^{+10}_{-9}	167^{+10}_{-9}
ξ [erg cm s^{-1}]	$\left(2.26^{+0.28}_{-0.20}\right) \times 10^3$	$(2.67 \pm 0.29) \times 10^3$
Fe/Fe$_\odot$	$3.4^{+1.6}_{-0.9}$	$2.8^{+0.8}_{-0.6}$
a	$-0.2^{+0.5}_{-0.4}$	0.22 ± 0.27
i[deg]	33 ± 4	24 ± 4
ϵ	$5.7^{+4.3}_{-2.0}$	3
χ^2/dof	392/313	398/314

References

Duro, R., Dauser, T., Wilms, J., et al. 2011, A&A, 533
Gou, L., McClintock, J. E., et al., 2011, ApJ
Sowers, J.W, Gies, D.R., Bagnulo,W.G., et al. 1998, ApJ506, 424
Davis R. & Hartmann, L. 1983, ApJ, 270, 671
Cadolle Bell, M. Sizun, P., et al., 2006, A&A, 446, 591